J|A|C|S COMMUNICATIONS

Published on Web 08/13/2010

Size Differentiation and Absolute Quantification of Gold Nanoparticles via Single Particle Detection with a Laboratory-Built High-Sensitivity Flow Cytometer

Shaobin Zhu, Lingling Yang, Yao Long, Min Gao, Tianxun Huang, Wei Hang, and Xiaomei Yan*

Department of Chemical Biology, College of Chemistry and Chemical Engineering, The Key Laboratory for Chemical Biology of Fujian Province, The Key Laboratory of Analytical Science, Xiamen University, Xiamen 361005, China

Received May 12, 2010; E-mail: xmyan@xmu.edu.cn

Abstract: Employing single nanoparticle detection with a laboratory-built high-sensitivity flow cytometer, we developed a simple and versatile platform that is capable of detecting the surface plasmon resonance scattering of gold nanoparticles (GNPs) as small as 24 nm, differentiating GNPs of different sizes, and providing accurate quantification of GNPs. Low-concentration samples (fM to pM) in small volumes (μL) can be measured in minutes with an analysis rate of up to 100−200 GNPs per second. Among these features, absolute quantification provides a distinct advantage because it does not require standard samples.

Gold nanoparticles (GNPs) have recently attracted enormous attention in medical, bioanalytical, and catalytic applications due to their unique optical, physical, and chemical properties.[1−3] Accurate size and concentration measurements of GNPs are vital to the quality control of GNP synthesis, surface functionalization, and assay development. Transmission electron microscopy (TEM) is the most commonly used method for GNP morphology characterization. Dynamic light scattering (DLS), an ensemble-averaged photon correlation approach, allows rapid and sensitive size measurement of GNPs but is limited to monodisperse samples and a scatter-free environment.[4,5] The size correlation of surface plasmon resonance (SPR) optical properties enables the analysis of GNP size, shape, and concentration in bulk measurements[6] and on single nanocrystals.[7] High-throughput spectral flow cytometers capable of acquiring surface enhanced Raman scattering spectra of individual plasmonic nanoparticles have recently been reported.[8,9] In contrast to the numerous methods for GNP size measurement, there is no efficient method for the accurate quantification of GNPs. The concentration of GNPs is usually calculated according to the GNP size measured by TEM and the gold content analyzed by inductive coupled plasma mass spectrometry (ICP-MS).[10] In addition to requiring expensive equipment, sample preparation is time-consuming.

Owing to the impressive signal-to-noise (*S*/*N*) ratio characteristic of confocal geometry, correlation spectroscopy of light scattering[11] and photothermal absorption[5] has been developed for the precise determination of the GNP hydrodynamic radius. In confocal systems, the laser beam is typically focused to a spot of 0.5 μm size defining a probe region of <1 fL. As the photon burst signals are collected from single particles that randomly diffuse in and out of the laser spot, a dramatic variation in scattering intensity of single bursts is commonly observed due to the Gaussian profile of the laser beam and the heterogeneity introduced by different trajectories taken by different particles through the excitation laser. However, the accurate counting of single GNPs is feasible once the GNP scattering signals can be unambiguously distinguished from the background noise. Reference GNP samples with known particle concentrations can be analyzed to build the calibration curve for GNP quantification.[12] Here, we apply a laboratory-built high-sensitivity flow cytometer (HSFCM)[13,14] for size differentiation and quantification of GNPs via single-particle detection.

HSFCM, also referred to as single molecule flow cytometry, employs hydrodynamic focusing of the sample in a sheath flow cuvette and then intersects the sample stream with a focused excitation laser beam.[15,16] Typically, subpicoliter probe volumes and millisecond transit times are used for background reduction and photon emission enhancement. If performed properly, the entire flow stream can be made to pass through the central region of the focused laser beam where irradiation is most uniform, and each nanoparticle flows through the apparatus at the same rate and experiences the same radiation as it traverses through the full width of the interrogation volume.[17] The detection of spherical polystyrene particles as small as 176 and 100 nm has been reported using side scattering detection within the sheath flow cuvette in 1987 and 2009, respectively.[13,18] Therefore, though the subpicoliter detection volume of HSFCM is inferior to confocal geometry for background reduction, it is possible to detect and differentiate single GNPs based on photon bursting due to the advantages of hydrodynamic focusing.

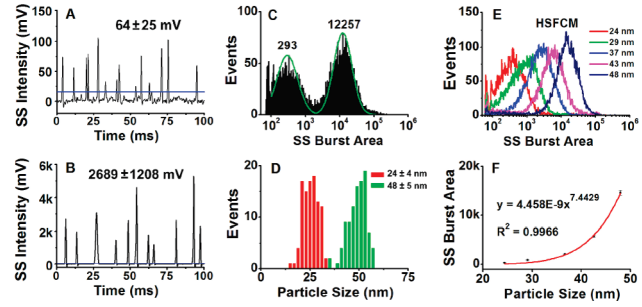

Figure 1. Flow cytometric analysis of single GNPs. (A and B) Typical side scatter (SS) burst traces (background corrected) of GNPs 24 and 48 nm in size, respectively. (C) SS burst area distribution histogram derived from a data set collected in 60 s intervals for a mixture of 24- and 48-nm GNPs. (D) Particle size distribution for samples of 24- and 48-nm GNPs as determined by TEM measurement. (E) SS burst area distribution histograms for five GNPs samples of different sizes. (F) Plot of measured SS burst area as a function of particle size.

A schematic diagram for the experimental arrangement is shown in Figure S1 (Supporting Information). Unlike the original setup,[13] this system used photomultiplier tubes for both the light scattering and fluorescence detection to make the instrument more compact and economical. The diameter of the focused laser beam was ~7.5 μm, and the diameter of the sample stream was ~5.0 μm. The detection

10.1021/ja104052c

volume was ~0.15 pL as defined by the overlap of the sample stream and the laser beam. The dwell time of single GNPs passing through the laser beam was ~1.5 ms. Figure 1A and 1B are representative traces of side scatter (SS) bursts of 24- and 48-nm GNPs, respectively. Due to the SPR effect, the intensity of Rayleigh scattering of each individual GNP can be satisfactorily discriminated from the background noise even for GNPs as small as 24 nm ($S/N = 22$). Nice SS burst area distribution histograms were obtained for the mixture of 24- and 48-nm GNPs with near-baseline separation (Figure 1C). TEM analysis (Figures 1D and S2) indicates that the broad distribution in SS burst area obtained on the HSFCM for all five GNP samples (Figure 1E) was mainly due to the size heterogeneity of the GNPs. According to the Mie theory, the intensity of light scattered by spheres that are much smaller than the wavelength of light is proportional to the sixth power of particle size. A plot of measured SS burst area versus particle size discloses a 7.4-order dependence (Figure 1D), which is in relatively good agreement with the theory. The high correlation between scatter intensity and particle size indicates that accurate size determination can be achieved by measuring the scattering intensity of single GNPs.

In our HSFCM setup, the sample stream was completely illuminated within the central region of the focused laser beam, and the radial diffusion of nanoparticles was negligible due to their small diffusion coefficients (~several $\mu m^2/s$).[11] Consequently, nearly 100% detection efficiency was demonstrated for 210-nm fluorescent polystyrene beads when the particle concentration was above 1×10^7 particles/mL.[13] Because the volumetric flow rate of the sample can be measured accurately (Supporting Information) as long as each individual GNP can be unambiguously resolved from the background, it is feasible to count the GNPs. However, precaution needs to be taken during enumeration to minimize the error introduced by the scattering bursts from impurity particles in the liquid medium. A typical burst trace of ultrapure water is displayed in Figure S3 with an average scattering burst rate of ~10 events per second. To demonstrate the capability of absolute quantification, 43-nm GNPs were diluted and analyzed on the HSFCM with sample concentrations ranging from 2.75×10^6 to 7.04×10^8 particles/mL. The background counts of water were subtracted from each GNP sample. Figure 2A displays an excellent linear relationship between the GNP concentrations determined by HSFCM and those calculated by the common TEM and ICP-MS approach. The correlation coefficient is 0.9998, and the linear range covers 2 orders of magnitude. Based on Poisson statistics, when the concentration of GNPs is 1.0×10^9 particles/mL (1.67 pM), the probability that two particles will happen to pass through the probe volume simultaneously is 0.96%. We note that the slope (0.9103) of the calibration curve deviated from 1.0. The systematic error between these two quantification methods could be ascribed to the inaccuracy of the TEM and ICP-MS approach due to the difficulty in calculating particle volume, which normally leads to deviation from the actual result.[12] This is also the first demonstration of the absolute quantification of GNPs.

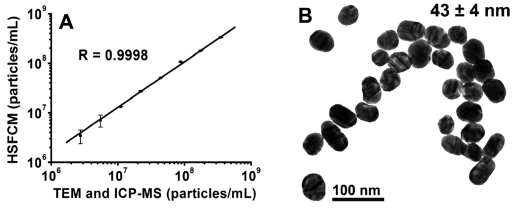

Figure 2. Absolute quantification of GNPs. (A) Linear relationship between GNP concentrations measured by HSFCM enumeration and by the TEM and ICP-MS approach. The error bars represent the standard deviation of three measurements. (B) TEM image of 43-nm GNPs.

Furthermore, the two-parameter (scattering and fluorescence) detection feature of HSFCM can be exploited to develop a simple quantification method using fluorescent nanoparticles as the internal standard. For a proof of principle, we mixed gold nanocrystals[19] with 210-nm fluorescent polystyrene beads (4.4×10^8/mL) in different ratios and then measured them on the HSFCM. As illustrated in the bivariate plot of fluorescence (FL) burst area versus SS burst area (Figure 3A), the particle mixture can be clearly distinguished into two populations based on the fluorescence signal, despite their comparable scattering intensity. An excellent linear correlation between the ratios detected by HSFCM and the theoretical ratios was obtained (Figure 3B). Therefore, accurate quantification of GNPs is feasible using the internal standard method.

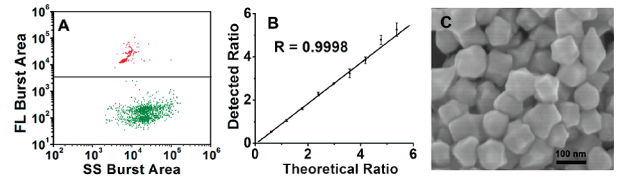

Figure 3. (A) Bivariate display of FL and SS burst area for a mixture of 120-nm gold nanocrystals with 210-nm fluorescent polystyrene beads. A line was drawn to facilitate discrimination. (B) Relationship between the ratios determined by HSFCM and the theoretical ratios. (C) SEM image of trisoctahedral gold nanocrystals.

In summary, employing single nanoparticle detection with a laboratory-built HSFCM, we developed a simple and versatile platform that is capable of detecting the SPR scattering of GNPs as small as 24 nm, differentiating GNPs of different sizes, and providing accurate quantification of GNPs. Low-concentration samples (fM to pM) in small volumes (μL) can be measured in minutes with an analysis rate of up to 100−200 GNPs per second. Among these features, absolute quantification provides a distinct advantage because it does not require standard samples. This is especially beneficial for nonfluorescent nanoparticles, most of which currently lack efficient quantification approaches.

Acknowledgment. This work was supported by the NSFC (20675070, 20975087, and 90913015), Program for New Century Excellent Talents in University (NCET-07-0729), Research Fund for the Doctoral Program of Higher Education of China (20090121120008), and NFFTBS (No. J0630429). We thank Dr. Qin Kuang of Xiamen Univ. for the supply of gold nanocrystals.

Supporting Information Available: Experimental details; Figures S1−S3. This material is available free of charge via the Internet at http://pubs.acs.org.

References

(1) Sperling, R. A.; Rivera Gil, P.; Zhang, F.; Zanella, M.; Parak, W. J. *Chem. Soc. Rev.* **2008**, *37*, 1896–1908.
(2) Hashmi, A. S.; Rudolph, M. *Chem. Soc. Rev.* **2008**, *37*, 1766–1775.
(3) Wilson, R. *Chem. Soc. Rev.* **2008**, *37*, 2028–2045.
(4) Liu, X.; Dai, Q.; Austin, L.; Coutts, J.; Knowles, G.; Zou, J.; Chen, H.; Huo, Q. *J. Am. Chem. Soc.* **2008**, *130*, 2780–2782.
(5) Octeau, V.; Cognet, L.; Duchesne, L.; Lasne, D.; Schaeffer, N.; Fernig, D. G.; Lounis, B. *ACS Nano* **2009**, *3*, 345–350.
(6) Njoki, P. N.; Lim, I. I. S.; Mott, D.; Park, H. Y.; Khan, B.; Mishra, S.; Sujakumar, R.; Luo, J.; Zhong, C. J. *J. Phys. Chem. C* **2007**, *111*, 14664–14669.
(7) Novo, C.; Funston, A. M.; Mulvaney, P. *Nat. Nanotechnol.* **2008**, *3*, 598–602.
(8) Sebba, D. S.; Watson, D. A.; Nolan, J. P. *ACS Nano* **2009**, *3*, 1477–1484.
(9) Goddard, G.; Brown, L. O.; Habbersett, R.; Brady, C. I.; Martin, J. C.; Graves, S. W.; Freyer, J. P.; Doorn, S. K. *J. Am. Chem. Soc.* **2010**, *132*, 6081–6090.
(10) Huang, C. C.; Chen, C. T.; Shiang, Y. C.; Lin, Z. H.; Chang, H. T. *Anal. Chem.* **2009**, *81*, 875–882.

(11) Kuyper, C. L.; Budzinski, K. L.; Lorenz, R. M.; Chiu, D. T. *J. Am. Chem. Soc.* **2006**, *128*, 730–731.
(12) Xie, C.; Xu, F.; Huang, X.; Dong, C.; Ren, J. *J. Am. Chem. Soc.* **2009**, *131*, 12763–12770.
(13) Yang, L.; Zhu, S.; Hang, W.; Wu, L.; Yan, X. *Anal. Chem.* **2009**, *81*, 2555–2563.
(14) Yang, L.; Wu, L.; Zhu, S.; Long, Y.; Hang, W.; Yan, X. *Anal. Chem.* **2010**, *82*, 1109–1116.
(15) Keller, R. A.; Ambrose, W. P.; Goodwin, P. M.; Jett, J. H.; Martin, J. C.; Wu, M. *Appl. Spectrosc.* **1996**, *50*, 12A–32A.
(16) Ambrose, W. P.; Goodwin, P. M.; Jett, J. H.; Van Orden, A.; Werner, J. H.; Keller, R. A. *Chem. Rev.* **1999**, *99*, 2929–2956.
(17) Van Orden, A.; Cai, H.; Goodwin, P. M.; Keller, R. A. *Anal. Chem.* **1999**, *71*, 2108–2116.
(18) Zarrin, F.; Risfelt, J. A.; Dovichi, N. J. *Anal. Chem.* **1987**, *59*, 850–854.
(19) Ma, Y.; Kuang, Q.; Jiang, Z.; Xie, Z.; Huang, R.; Zheng, L. *Angew. Chem., Int. Ed.* **2008**, *47*, 8901–8904.

JA104052C